


**Research Article**

## pXRF, Raman, and Multivariate Analysis Aiming to Discriminate Among Different Kinds of Marble Fragments of “Hygeia” Sculpture from Museu de Arte de São Paulo Assis Chateaubriand’s Collection

Leticia Martins Birelo<sup>1\*</sup>, Rafael Molari<sup>1</sup>, Carlos Roberto Appoloni<sup>1</sup>, Lilian de A. Laky<sup>2</sup>

### Abstract

The marble statue of Hygeia (1st–2nd centuries AD), part of the collection of the Museu de Arte de São Paulo Assis Chateaubriand (MASP), is believed to have undergone extensive restoration in 18th-century Rome. The sculpture, composed of 185 fragments and measuring 161 cm in height, represents a complex assemblage of original ancient elements and later additions. In this study, a fully non-destructive analytical approach combining portable X-ray fluorescence (pXRF), Raman spectroscopy, and multivariate statistical analysis was applied to investigate the material composition of selected fragments. Twenty regions of the statue were analyzed in situ and compared with three reference marbles of known provenance: Paros, Pentelikon, and Thasos. Elemental and molecular data were evaluated using Principal Component Analysis (PCA) and Hierarchical Cluster Analysis (HCA). The multivariate results consistently separate the analyzed regions into two main groups, in agreement with independent stylistic and archaeological assessments. Furthermore, the combined spectroscopic and statistical evidence indicates compositional affinity with Paros and Pentelikon marbles, while allowing Thasos marble to be excluded. These results demonstrate that the integration of non-invasive spectroscopic techniques with multivariate analysis is an effective strategy for addressing questions of material characterization and restoration history in archaeological sculptures when sampling is not permitted.

**Keywords:** Statue; Hygeia; Non-destructive analysis; Multivariate analysis.

### Introduction

The currently employed techniques for studying cultural heritage are non-destructive and utilize various parts of the electromagnetic spectrum to gather valuable information about elemental and chemical compositions, conservation states, and potentially the artist’s creative process. Many studies in literature apply various techniques to identify the provenance, physical and chemical characteristics of marbles, emphasizing a non-destructive, multi-technique approach [1–28]. Roman white marble fragments have been characterized using petro-archaeometric analysis to determine their provenance, with mineralogical and chemical analyses performed using X-ray Diffraction and portable X-ray Fluorescence [1]. It was also possible to characterize granitoid statues to identify their materials and provenance, although this can be challenging due to their fine-grained nature and dark color [2].

### Affiliation:

<sup>1</sup>Applied Nuclear Physics Laboratory, Physics Department, State University of Londrina (UEL), 86057-970, Londrina, PR, Brazil

<sup>2</sup>Museum of Archaeology and Ethnology, University of São Paulo (USP), São Paulo, Brazil

### \*Corresponding author:

Leticia Martins Birelo, Applied Nuclear Physics Laboratory, Physics Department, State University of Londrina (UEL), 86057-970, Londrina, PR, Brazil.

**Citation:** Leticia Martins Birelo, Rafael Molari, Carlos Roberto Appoloni, Lilian de A. Laky. pXRF, Raman, and Multivariate Analysis Aiming to Discriminate Among Different Kinds of Marble Fragments of “Hygeia” Sculpture from Museu de Arte de São Paulo Assis Chateaubriand’s Collection. *Journal of Analytical Techniques and Research*. 8 (2026): 16–26.

**Received:** March 16, 2026

**Accepted:** March 23, 2026

**Published:** March 31, 2026

Multi-technique analysis has also been employed on religious wooden statues such as the “Virgin with Child,” “Saint Lucy,” “Saint Sebastian,” and “Our Lady of Conception” [3-5]. In these studies, in addition to X-ray Fluorescence, techniques such as Radiography, Computed Tomography, Near-Infrared, Pulse Thermography, Holographic Interferometry, and Scanning Electron Microscopy were used to identify internal issues, damages, retouches, and the materials and pigments used by the artists. Although these examples differ in material composition, they illustrate the versatility of non-destructive, multi-technique approaches in cultural heritage research and their applicability to complex, heterogeneous artworks such as marble sculptures.

Techniques such as X-ray Fluorescence, Raman Spectroscopy, and ATR-FTIR could also be combined to identify pigments, as demonstrated in studies of three seated statues from the Torreparedones archaeological site [6] and the “Pietà” of Barletta [7], where different shades and intensities of yellow, red, and blue pigments were observed. Additionally, non-invasive and invasive analyses have been combined to study alterations in marble statues to better understand the sources of brown chromatic changes that have occurred [8].

The sculpture of Hygeia was acquired by the Museu de Arte de São Paulo (MASP) at the auction of the antiquity collection of William Lowther, 2nd Earl of Lonsdale (1848 and 1868), from Lowther Castle in England in 1947. The first English collection Hygeia belonged to was William Ponsonby (1704-1793), the 2nd Earl of Bessborough, or Lord of Duncannon. Hygeia arrived in England in the 18th century through the hands of Thomas Jenkins and Charles Townley, who acquired it in Bologna, Italy, from the collection of the Marquis of Locatelli, which was disposed of after his death. The sculpture of Hygeia was found in the Statilii theatre in the area of the church of Santa Croce in Jerusalem in Rome by Carlo Albacini, who restored it. He was a restorer at Bartolomeo Cavaceppi's workshop in Rome (Bignamini & Hornsby, 2010:156). It is known this from the letter Thomas Jenkins wrote to Charles Townley on July 3, 1784, which details the sculpture and reveals the identity of its Italian restorer [9]. Michaelis only provided the information that it was carved from Paros marble in the 19th century [11]. No further studies have attempted to elucidate the marble origin of Hygeia from MASP [10].

The sculpture of Hygeia comprises 185 fragments, measuring 161 cm in height (152 cm excluding the base) and 70 cm x 58 cm in width and depth (Figure 1). Not all these fragments are part of the statue elaborated in antiquity. The difference between the dark marble (called type I), the oldest, and parts of the lighter marble (type II), the most recent, indicates, as we already know, interventions in the sculpture

made when it was reassembled in modern times [10]. Despite this, the main parts of the statue, which are original, such as the head and the entire front, side, and back of Hygeia, are complete [10]. Regarding the parts added to the sculpture during the restoration in the 18th century, the preliminary visual examination was inconclusive in some parts of the statue: part of Eros's body, the stretch from the thighs to the waist, and the right forearm on which the coiled serpent lies. The arm and the final section of the serpent are indeed part of the ancient sculpture. Still, it was not possible to conclude, through visual examination, whether all the rest (the forearm, the rest of the serpent's body and head, and Hygeia's hand) is ancient or was carved from another marble and added during the restoration. Some of these parts were analyzed using portable X-ray fluorescence (pXRF) and Raman spectroscopy, as described below. This work presents a case study with an integrated analysis of the Greek marble statue of Hygeia, part of the Museu de Arte de São Paulo Assis Chateaubriand (MASP) collection, aiming to assess the similarity between the statue's marble fragments among themselves, and also relate them with three non-archaeological marble samples — Paros, Pentelikon, and Thasos. The goal was to determine whether the statue fragments originated from the same kind of marble or if additional types of marble were introduced into the piece. Due to the museum's collection policies, sampling was not allowed.

## Materials and Methods

The Hygeia statue analyzed in this study is shown in Figure 1. In situ portable X-ray fluorescence (pXRF) and Raman spectroscopy measurements were taken at 20 points using a pXRF system developed by the Applied Nuclear Physics Laboratory (LFNA) at the State University of Londrina (UEL) [29] and the Inspector Raman by DeltaNu. The portable XRF system consisted of a mini X-ray tube from Moxtek Inc. (4 W power, 10–40 kV voltage, and 0–100  $\mu$ A current) with a silver (Ag) anode, along with the X-123SDD Complete X-Ray Spectrometer with Silicon Drift Detector from Amptek Inc., equipped with a 3 mm silver (Ag) collimator. The angle between the X-ray tube and the detector was 90°, and a pair of low-intensity lasers was integrated to pinpoint the area under analysis. The system head was fixed, and the nominal distance between the equipment and the statue was approximately 1 mm. However, due to the irregular surface of the statue, slight variations in distance were inevitable. The experimental setup was optimized to minimize dead time. For the statue measurements, the X-ray tube was operated at 28 kV and 4  $\mu$ A, while for the reference standards, a lower current of 1.5  $\mu$ A was used to prevent detector saturation. No filter was employed. Each spectrum was collected over 500 seconds. Spectral analysis was carried out using WinQXAS software provided by the International Atomic Energy Agency [30].



**Figure 1:** Statue of Hygeia from MASP, comprising 185 fragments, 161 cm in height (152 cm excluding the base) and 70 cm x 58 cm in width and depth.

In situ Raman spectroscopy was performed on the Hygeia statue using the DeltaNu Inspector Raman system, that was calibrated before all measurement sets were performed using the reference material in accordance with the manufacturer's instructions. The system employed a 785 nm laser with a resolution of less than  $8\text{ cm}^{-1}$ . The spectral range covered  $200\text{ cm}^{-1}$  to  $2000\text{ cm}^{-1}$ , with each spectrum acquired over 3 seconds and averaged over ten integrations. Spectral acquisition was carried out using the NuSpec software. Additionally, three marble samples of known provenance — Paros, Pentelikon, and Thasos — were analyzed using both pXRF and Raman spectroscopy.

Formultivariate analysis, MATLAB version 9.12(R2022a) was used, applying Principal Component Analysis (PCA) and Hierarchical Cluster Analysis (HCA) to spectroscopic data. The pXRF data were preprocessed using autoscale, while the Raman data underwent mean-centering, and for both analyses it was used the Euclidean metrics and specifically for HCA it was used Ward's method. The analyzed points on the statue are distributed in different regions of the state, such as in the cloth (P1, P2, P3, P4, P5, P6, P11, P16, and P17), snake (P7 and P8), right hand (P9 and P10), phiale (P12), Eros (P13, P14, and P15), and face (P18, P19, and P20). Some of these regions are shown in detail in Figure 2.



**Figure 2:** Analyzed points in Hygeia's (a) face, (b) Eros and phiale, (c) snake and right hand, and (d) cloth, due to diagnostic stylistic features.

## Results and Discussions

### Stylistic Analysis or Archaeological and Historical Data

There is no doubt that this is a sculptural type of Hygeia, given the 18th and 19th century reports [11, 14] on the serpent portion belonging to the original arm of the statue, which is in line with the conclusions of the stylistic research. The style of the sculpture (the features of the face, the garments, the design of the whole body, and its positioning) reveals the period in which the statue was made (1st-2nd AD); however, the characteristic hairstyle is the main iconographic element that we have to date. It is a hairstyle characteristic of statues of Hygeia dating from the 2nd century AD [10]. About Eros, although the god was depicted next to the statues of Hygeia from the 2nd-3rd centuries AD, in the MASP sculptural type, he does not belong to the original statue from Antiquity but was most likely added by restorers in the 18th century, using parts of ancient different sculptures.

### pXRF and Raman Analysis

The pXRF data collected from 20 regions of the sculpture, along with the spectra from the three known marble types — Paros (Pa), Pentelikon (Pe), and Thasos (Th) — proved difficult to analyze. To analyze the spectra with WinQXAS, each spectrum was segmented into five distinct regions. Due to a limitation of this software, it was not possible to perform a fit on the entire spectrum, as it contained elements with intense peaks, which can be up to three orders of

magnitude higher when compared to minor elements with low intensities. The first region includes low-energy elements (Si, S, Cl, Ar, K, and Ag-L $\alpha$ ); the second region focuses on the K $\alpha$  and K $\beta$  lines of Ca; the third region highlights peaks from Ti, Mn, and Fe; the fourth region covers peaks from Cu, Zn, and Pb-L $\alpha$ ; and the fifth region emphasizes the K $\alpha$  line of Sr. Figure 3a presents the overlapping of all pXRF spectra. An attempt was made to maintain 1 mm distance between the detector collimator's output and the sample. However, this was not possible at all points due to surface irregularities, which can be clearly observed in Figure 1. For this reason, normalization was performed using the argon (Ar) peak, as its area is proportional to the thickness of the air layer between the detector and the sample. This approach, currently employed in the literature, directly accounts for variations in distance, ensuring that, once normalized to the Ar peak, all measurements are adjusted to a single reference [12, 13]. The Ar normalization was applied to compensate for variations in detector-sample distance caused by surface regularities. While increased air gaps attenuate both characteristic X-rays from the sample and enhance the Ar signal, normalization to Ar provides a first-order correction widely adopted in in situ pXRF studies. As the measurements on the statue and the marble samples were performed with different acquisition parameters — 4  $\mu$ A for the statue and 1.5  $\mu$ A for the marbles — it was necessary to normalize the elements net intensities by current (cps/ $\mu$ A).

Raman measurements were also carried out at the same 20 points on the statue and the three marble samples. Raman spectral analysis, performed using Origin 2018 (version 95E), revealed intense calcite bands at  $\sim$ 1085  $\text{cm}^{-1}$ ,  $\sim$ 715  $\text{cm}^{-1}$ , and  $\sim$ 287  $\text{cm}^{-1}$ , along with a gypsum band at  $\sim$ 1005  $\text{cm}^{-1}$  and an amorphous carbon  $\sim$ 1323  $\text{cm}^{-1}$  [16], as seen in Figure 3b. The strong calcite bands in the Raman spectra overshadowed weaker signals, which made it difficult to visualize differences between the statue and the three marble samples, which could be verified only by the multivariate analysis. Since all Raman spectra were similar, no differences could be identified between the statue's regions and the measured marble standards.

### Multivariate Analysis

With all spectroscopic analyses performed, multivariate analyses such as Principal Component Analysis (PCA) [31] and Hierarchical Cluster Analysis (HCA) [32] were performed. For data treatment, it was used the package of tools PLS\_Toolbox version 9.0, together with the software MATLAB version 9.12 (R2022a). The initial point for PCA is the data matrix for pXRF measurements, presented in Table 1, where the lines correspond to the 23 analyzed regions, and the columns represent the intensities of the identified elements. For Raman measurements, it was also necessary to

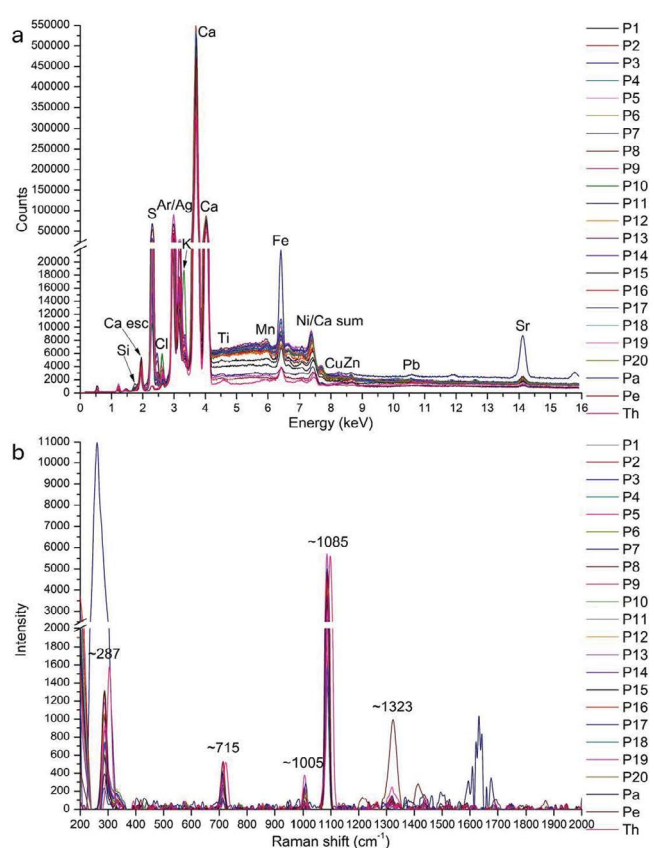


**Figure 3:** (a) Overlapping of all pXRF spectra and (b) Raman spectra highlighting the principal bands of calcite, gypsum and amorphous carbon.

construct a table where the lines correspond to the 23 analyzed regions, and the columns show the Raman Shift ( $\text{cm}^{-1}$ ) from 200  $\text{cm}^{-1}$  to 2000  $\text{cm}^{-1}$ . Principal Component Analysis (PCA) was applied to reduce the dimensionality of the spectroscopic datasets and to identify patterns of similarity among the analyzed points. Score plots represent the distribution of samples in the reduced variable space, while loading plots indicate the contribution of each variable to the observed separation. Hierarchical Cluster Analysis (HCA) was used as a complementary tool to visualize sample grouping and confirm clustering trends.

First, HCA and PCA for the pXRF analysis points considered all the variables in the analysis. Figure 4 shows the dendrogram for HCA, and scores and loadings of PC1xPC2. It is possible to observe that P10 is an outlier, which is why it is removed from the grouping analysis. Successive PCA and HCA analyses were performed to evaluate the robustness of the observed groupings, to assess the influence of outliers and dominant variables on sample separation and also compare with the results of the stylistic analysis.

Maybe P10 must have a different composition from other regions of the sculpture. Figure 5 shows the scores and

**Table 1:** Identified inorganic elements normalized net intensities (cps/ $\mu$ A).

	Si	S	Cl	K	Ca	Ti	Mn	Fe	Cu	Zn	Sr	Pb
P1		112.77	2.78		2404.69	1.28	4.05	30.75		1.80	5.13	3.43
P2		199.46	3.30		4028.87		6.50	34.30	3.94	4.35	8.46	
P3		278.09	9.50		5174.12	2.99	9.79	68.56		6.45	12.28	8.89
P4		242.93	8.97		4988.66		8.45	59.07	2.76	10.90	12.64	6.82
P5		207.33	8.58		10495.48		9.95	79.19		4.96	15.29	25.96
P6		376.11	17.55		9401.02		22.74	56.31		3.55	16.40	19.77
P7		530.92	29.84		4017.08	5.12	27.91	209.61		7.28	111.02	7.68
P8		373.48	10.12		4110.05		13.64	40.17	2.15	6.82	11.77	3.78
P9		214.16	40.50	11.38	8153.16	1.67	18.91	39.12	5.44	16.13	16.13	
P10	14.09	372.63	164.47	380.07	23218.22	44.96	14.10	181.14	9.37	42.93	42.49	
P11		198.80	22.58		8366.65	4.33	14.63	32.85		13.02	13.27	
P12		269.74	22.28	4.64	8221.95		11.84	35.29		18.26	15.97	7.35
P13		475.24	17.44		11063.69		38.00	67.81		22.49	20.19	7.74
P14		401.19	9.09	11.25	8345.88		12.46	46.03	4.60	17.78	14.79	
P15		89.09	3.05		2475.29		2.22	20.23		1.01	3.71	1.77
P16		192.65	3.89		6377.70		4.22	10.24			11.24	
P17		265.65	7.80		7591.78		8.22	41.56		8.17	15.94	8.31
P18		270.08	11.66		8004.03		11.47	20.10		8.92	18.08	9.54
P19		58.61	1.40	4.17	1076.88	0.42	1.07	5.85	0.88	2.57	2.37	1.02
P20		368.60	8.51		8353.33		21.69	47.75		9.23	17.97	7.64
Pa	1.73		7.26		5379.95	5.99		12.89		21.41	5.37	3.48
Pe	3.15		1.85	7.82	4356.04	2.38		16.81	3.28	5.42	2.90	2.95
Th	1.47	1.78	7.91	3.88	2312.45	4.91	1.90	18.47		6.90	1.14	1.81

loadings for PC1xPC2 and the dendrogram for HCA excluding P10. The marble samples group with each other, and some points form two distinct groups. The analysis was performed considering all detected elements; Ar that did not belong to the sculpture was maintained because its intensity was the same for all points and did not interfere with the sample grouping. The identification of this outlier do not necessarily indicate a different provenance but rather highlights localized compositional variability or surface-related effects, which are expected in *in situ*, non-invasive measurements.

A new analysis was performed excluding calcium, due to its high intensity and low discriminatory power, and lead, which may originate from surface contamination or restoration-related materials rather than from the intrinsic marble composition, possibly as a result of accumulated environmental pollution. This revised analysis is shown in Figure 6. Once again, the marble samples cluster together, with some data points forming two distinct groups.

Studies, such as reference [15], have demonstrated that the Fe/Sr ratio can be used to differentiate marble samples. The results presented in Figure 7 reinforce this finding, showing

that only the Thasos marble (Th) exhibits a distinct Fe/Sr ratio. In contrast, the other two marbles (Pa and Pe) display similar values, aligning with the overall behavior observed across all measured regions of the sculpture. This suggests that, based on the Fe/Sr ratio, the sculpture's marble is more consistent with Pa and Pe, further supporting our material characterization.

The Fe/Sr ratio is used here as an indicative compositional parameter to support comparative analysis among samples. Its main contribution is the clear distinction of Thasos marble, while Paros and Pentelikon exhibit overlapping values consistent with the multivariate results. For Raman measurements, PCA and HCA considered all the spectra of the statue points and the marbles samples. Figure 8 shows the dendrogram, scores and loadings plot for PC1xPC2 with an 87.59% explained variance. PCA for all points show that P7 is an outlier, and the sample of Thasos marble is not similar with the other samples, as also shown in the Fe/Sr ratio graph. The Fe/Sr ratio is used only as an indicative parameter to compare the measured regions of the sculpture with reference marbles, rather than as a definitive provenance marker. The Fe/Sr ratio provides supportive evidence that helps exclude Thasos

marble, while highlighting the compositional similarity between the sculpture and Paros/Pentelikon marbles. The loading plot shows the principal bands of calcite near 261  $\text{cm}^{-1}$  and 1089  $\text{cm}^{-1}$  as key factors in the separation. The HCA exposes P7 as an outlier.

Since P7 is an outlier in Raman analysis, it was removed from the PCA to assess any differences. The new accumulated variance for PC1xPC2 was 76.86%, the new plot of scores and loadings and the new dendrogram for HCA are shown in Figure 9.

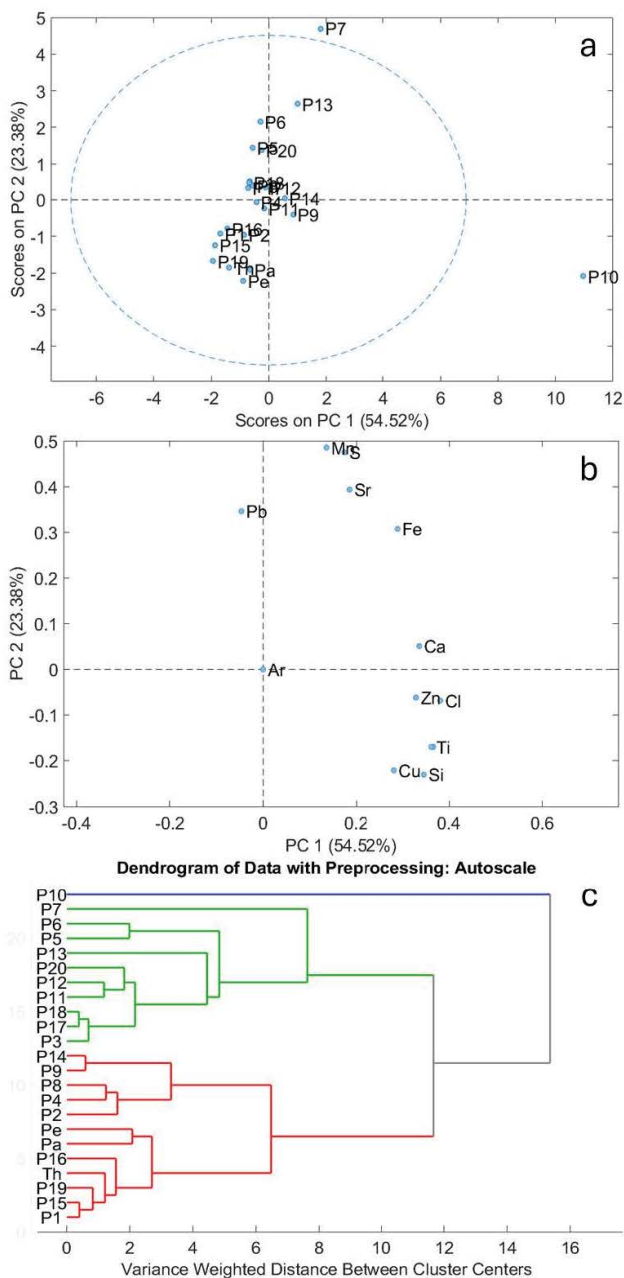


**Figure 4:** (a) Scores and (b) loadings of PC1xPC2 and (c) dendrogram for HCA, for the pXRF measurements.

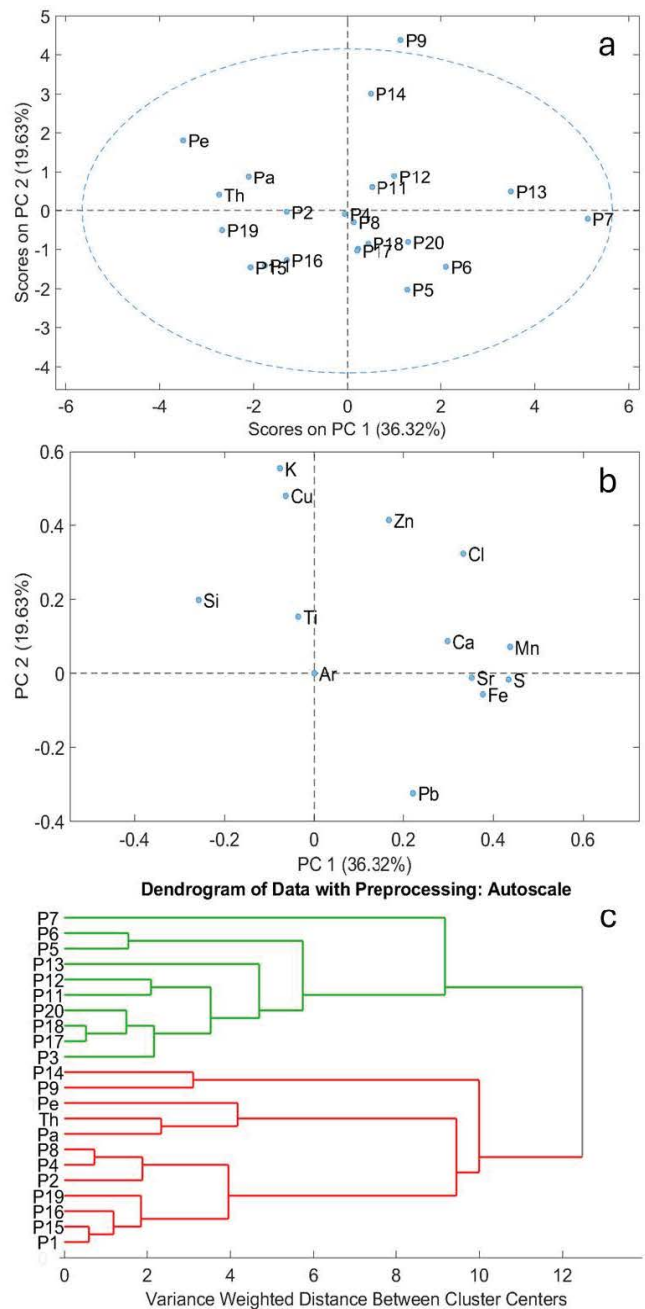


**Figure 5:** (a) Scores and (b) loadings of PC1xPC2 and (c) dendrogram for HCA, for the pXRF measurements excluding P10.

Marble Thasos appeared now as an outlier, reinforcing the conclusion from the Fe/Sr ratio graph, showing that this sample does not present any compositional similarity with the fragments nor with the other two marble samples. So, last but not least, removing Thasos marble from the multivariate analysis, it is possible to see, in Figure 10, the scores and loadings for PC1xPC2 with a total of 80.21% of the accumulated variance, and the dendrogram for HCA. Now, there are two-point groups, where Pentelikon and Paros

samples group with each other. The identification of these two outliers, P7 and Thasos marble, in Raman analysis does not necessarily indicate a different provenance but rather highlights localized compositional variability or surface-related effects, which are expected in in situ, non-invasive measurements, just as in pXRF analysis.

Based on the above, it can be verified that, particularly considering the Raman measurements, the multivariate analysis separates the marble fragments of the statue into two

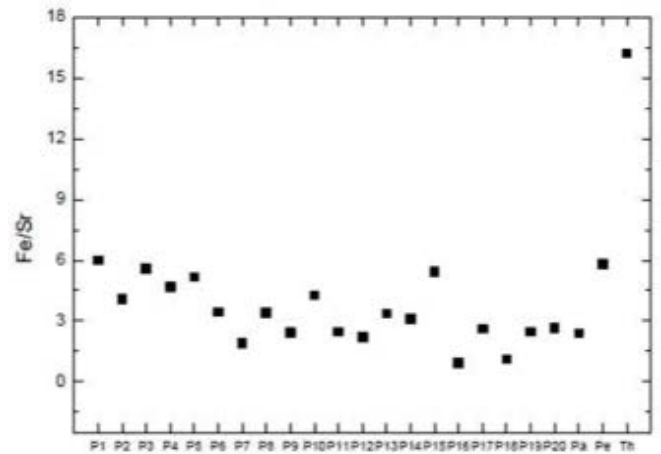


Figure 7: Fe/Sr ratio for the points in Hygeia's statue and the marble samples.

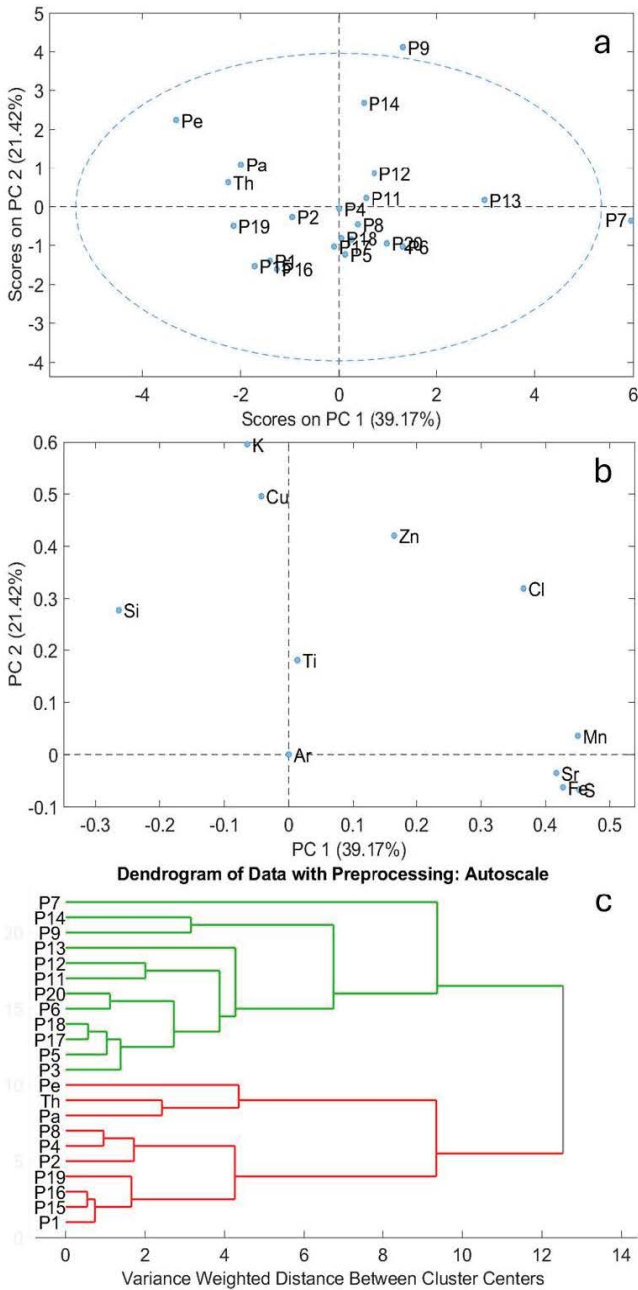


Figure 6: (a) Scores and (b) loadings of PC1xPC2 and (c) dendrogram for HCA, for the pXRF measurements excluding P10, calcium and lead.

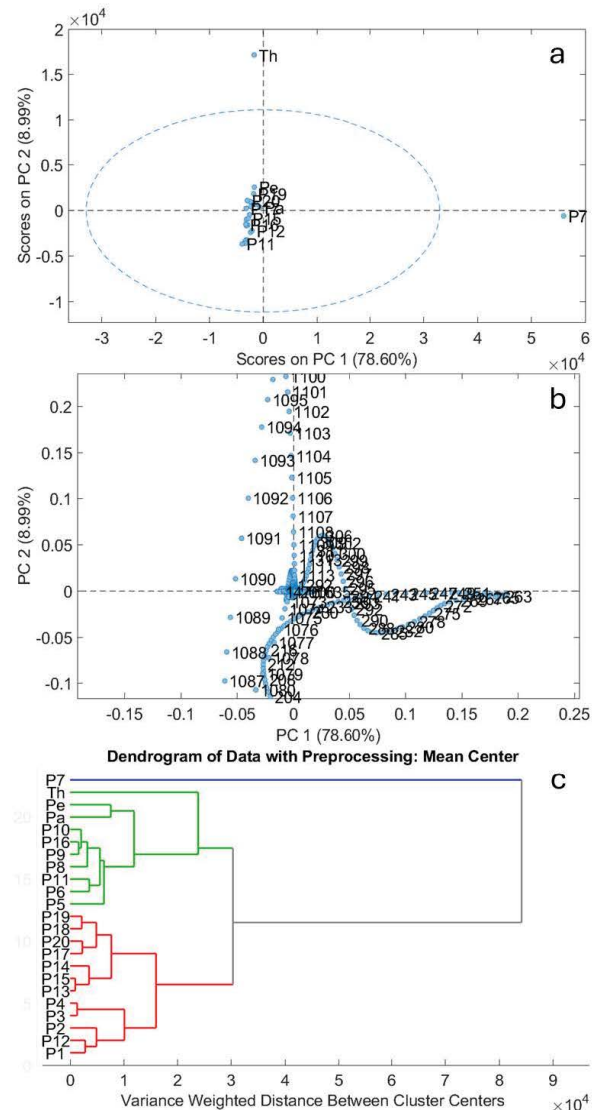
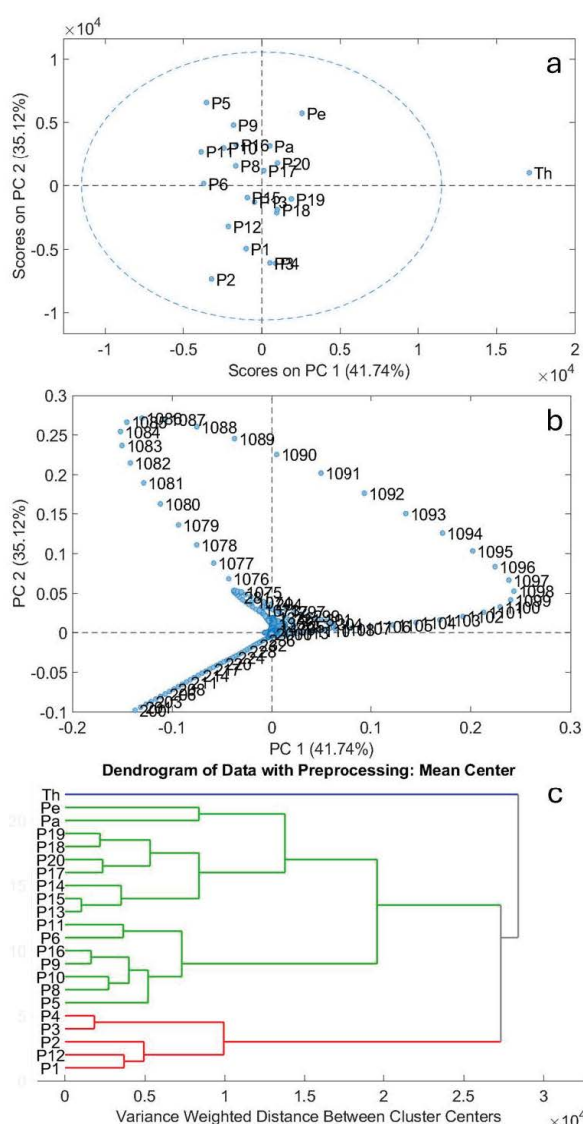


Figure 8: Plot of (a) scores and (b) loadings of PC1xPC2 and (c) HCA for Raman measurements.



**Figure 9:** Plot of (a) scores and (b) loadings of PC1xPC2 and (c) HCA for the Raman measurements removing P7.

distinct groups. The smaller group comprises the fragments corresponding to the garment (P1, P2, P3, and P4) and the vessel (P12), in agreement with the independent stylistic and archaeological analysis. Furthermore, there are strong evidence that the marbles used bear similarities to marbles Paros and Pentelikon and differ from marble Thasos.

## Conclusions

The integration of pXRF, Raman spectroscopy, and multivariate analysis proved particularly effective for non-invasive investigation of archaeological marbles. These techniques are well established for identifying subtle geochemical differences, even when destructive sampling is not permitted, offering robust data for provenance and restoration studies. Despite the limitations imposed

by museum policies prohibiting sampling, the adopted methodology successfully provided compositional and mineralogical information. The normalization procedures and multivariate approach mitigated variations arising from surface irregularities and measurement geometry.

Multivariate analysis, PCA, and HCA for pXRF and Raman spectra separated the marble fragments into two groups, confirming the results of the stylistic/archaeological analysis, which was performed independently, in parallel, and without communication with the spectroscopic analysts. Although differences among reference marbles (Paros, Pentelikon, Thasos) were observed, these may reflect surface conditions and measurement constraints inherent to in situ analyses. Considering the complementary archaeological and stylistic evidence, the results still suggest that Paros and Pentelikon marbles are the most consistent sources, while acknowledging that a definitive provenance determination would require sampling and additional analyses. As a future work it would be recommended to do some additional analysis such as C-13 and O-18 isotopes analyses to obtain more information about the provenance of the marbles in the statue, but it would be necessary to take samples that was not possible for this study, due to sampling restrictions.

The agreement between these methodologies highlights the robustness of the findings. The statistical treatment played a key role in integrating pXRF and Raman datasets, enhancing the discrimination capability of the analysis and revealing subtle groupings that align with independent stylistic assessments. These results not only validate the use of non-destructive techniques in the study of cultural heritage but also provide a solid foundation for future research on the characterization of this kind of archaeological material. The results are consistent with Michaelis' historical hypothesis regarding the possible use of Parian marble; however, they should be interpreted as supportive evidence rather than definite proof, given the exclusively non-invasive nature of the analyses. It is important to highlight that these results are from XRF and Raman portable measurement systems that are noninvasive and non-destructive; however, these techniques have limitations. The ideal would be to take some samples to measure in an EDXRF or WDXRF system in a vacuum chamber, just like performing X-ray diffraction (XRD), but this was not allowed.

## Author Contributions

“Conceptualization, Carlos R. Appoloni. and Lilian de A. Laky; Methodology, Carlos R. Appoloni and Lilian de A. Laky.; Validation, Leticia M. Birelo, Carlos R. Appoloni and Rafael Molari; Formal analysis, Leticia M. Birelo, Carlos R. Appoloni and Rafael Molari; Investigation, Leticia M. Birelo, Carlos R. Appoloni, Rafael Molari and Lilian de A. Laky; Resources, Carlos R. Appoloni and Lilian de A. Laky; Data

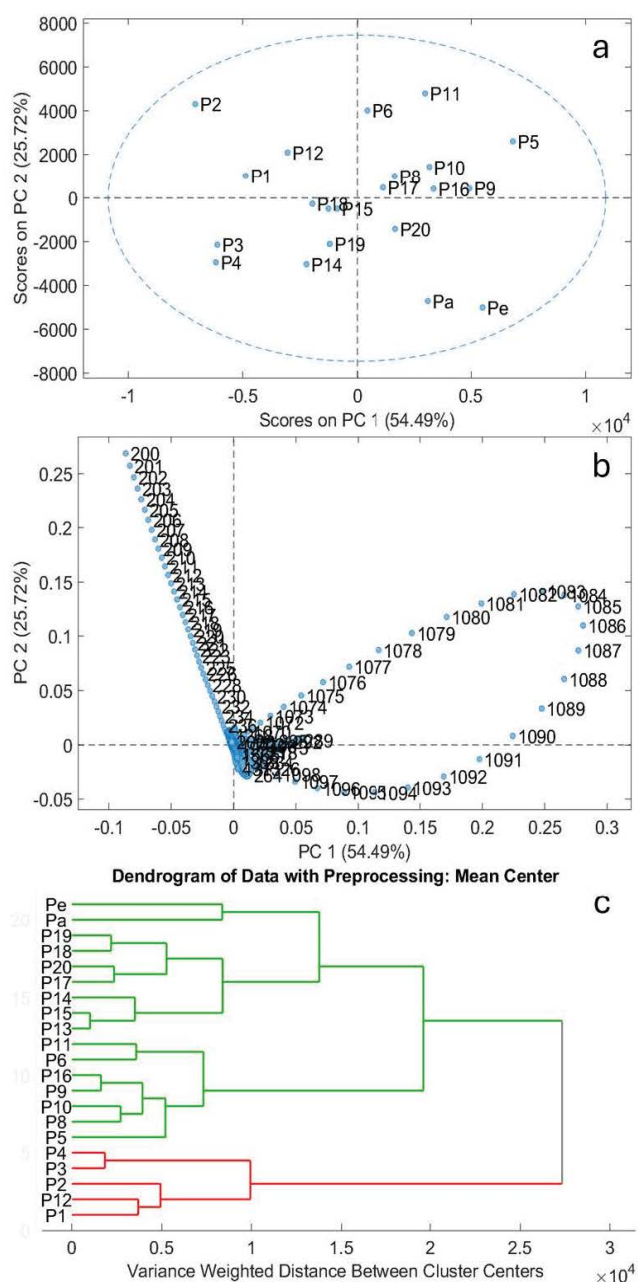


**Figure 10:** Plot (a) scores and (b) loadings of PC1xPC2 and (c) HCA for Raman measurements removing the marble Thasos.

curation, Leticia M. Birelo, Carlos R. Appoloni and Rafael Molari; Writing — original draft preparation, Leticia M. Birelo, Carlos R. Appoloni, Rafael Molari and Lilian de A. Laky; Writing — review and editing, Leticia M. Birelo, Carlos R. Appoloni, Rafael Molari and Lilian de A. Laky; Visualization, Carlos R. Appoloni and Lilian de A. Laky; Supervision, Carlos R. Appoloni and Lilian de A. Laky; Project administration, Carlos R. Appoloni and Lilian de A. Laky; Funding acquisition, Carlos R. Appoloni and Lilian de A. Laky.

## Acknowledgments

The authors would like to acknowledge the Museu de Arte de São Paulo team for making this work possible, in particular the collection team for all support during the pXRF and Raman measurements. The National Council for Scientific and Technological Development (CNPq), Brazilian Federal Agency for Support and Evaluation (CAPES) and the National Institute of Science and Technology: Nuclear Physics and Application (INCT-FNA). We thank Mr. Yannis Kourayos for providing the marble sample from Paros. This research was part of the project *The sculpture of Hygeia from the MASP collection: an iconographic and contextual study*, funded by MASP Research Program between 2016 and 2017, coordinated by Dr Lilian de A. Laky.

## Reference

1. G. Barone N, Bruno A, Giuffrida P, et al. Achaometric investigation of a Late Roman marble statue from Kaucana (RG) with considerations on the diffusion of Thasos marble in Sicily. *Periodico di Mineralogia* 2 (2013): 313-329.
2. S Müskens, D Braekmans, M J Versluys, et al. Egyptian sculptures from Imperial Rome. Non-destructive characterization of granitoid statues through macroscopic methodologies and in situ XRF analysis. *Archaeol Anthropol Sci* 10 (2018): 1303-1318.
3. S Sfarra, C Ibarra-Castanedo, S Ridolfi, et al. Holographic Interferometry (HI), Infrared Vision and X-Ray Fluorescence (XRF) spectroscopy for the assessment of painted wooden statues: a new integrated approach. *Applied Physics A* 115 (2014): 1041-1056.
4. C Calza, D F Oliveira, R P Freitas, et al. Analysis of sculptures using XRF and X-ray radiography. *Rad Phys Chem* (2015): 326-331.
5. R Oliveira, A de Paula, F Gonçalves, et al. Analysis of a wooden statue by non-destructive X-ray techniques. *X-ray Spectrometry* (2022).
6. D Cosano, L D Mateos, C Jiménez-Sanchidrián, et al. Identification by Raman microspectroscopy of pigments in seated statues found in the Torreparedones Roman archaeological site (Baena, Spain). *Microchemical Journal* (2017): 191-197.
7. D Marano, I M Catalano, A Monno. Pigment identification on “Pietà” of Barletta, example of Renaissance Apulian sculpture: A Raman microscopy study. *Spectrochimica Acta Part A* (2006): 1147-1150.
8. D Pinna, M Galeotti, A Rizzo. Brownish alterations on the marble statues in the church of Orsanmichele in Florence: what is in their origin? *Heritage Science* 3 (2015): 7.

9. Bignamini, C Hornsby. Digging and dealing in Eighteenth century Rome. Yale University Press 2 (2010).
10. L A Laky. A escultura de Higeia do acervo do MASP: um estudo contextual e iconográfico. MASP Research Program (final scientific report). São Paulo (2017).
11. MICHAELIS. Ancient marbles in Great Britain. Cambridge (1882).
12. T Cramer, J C Molano, A D Öcal. Provenance determination of archaeological marbles as example for the use of geoscientific methods in archaeometry. *Geologia Colombiana* 35 (2010): 143-161.
13. Arjonilla P, Domínguez-Vidal A, de la Torre López M J, et al. In situ Raman spectroscopic study of marble capitals in the Alhambra monumental ensemble. *Appl. Phys* 122 (2016): 1014.
14. Ahmad A, and Al-Bashaireh K. Provenance Determination and Condition Assessment of Archaeological Marble Statues from Gerasa Using Non-Destructive Ultrasonic Technique. *Studies in Conservation* 66 (2021): 397-412.
15. Saltarelli C, Rippa M, Pagliarulo V, et al. The heritage Building Information Modelling System for non-destructive optical techniques: The case study of the restoration of a Marble sculpture on the façade of the Gesù Nuovo Church in Naples. *Acta IMEKO* 14 (2025): 1.
16. Ahmad A. Investigation of Marble Deterioration and Development of A Classification System For Condition Assessment Using Non-Destructive Ultrasonic Technique. *Mediterranean Archaeology and Archaeometry* 20 (2020): 2241-8121.
17. Sáez-Pérez M P, Durán-Suárez J A, Castro-Gomes J. Study of the correlation of the mechanical resistance properties of Macael white marble using destructive and non-destructive techniques. *Construction and Building Materials* 418 (2024).
18. Menningen J, Siegesmund S, Krompholz R, et al. The marble sculptures of General Bülow and Scharnhorst in Berlin: comparative, non-destructive analysis of the weathering state after 12 years of exposure. *Environ Earth Sci* 249 (2020).
19. Ion RM, Bakirov B A, Kichanov S E, et al. Non-Destructive and Micro-Invasive Techniques for Characterizing the Ancient Roman Mosaic Fragments. *Appl. Sci* 10 (2020): 3781.
20. Macchia A, Cerafogli E, Rivaroli L, et al. Marble Chromatic Alteration Study Using Non-Invasive Analytical Techniques and Evaluation of the Most Suitable Cleaning Treatment: The Case of a Bust Representing Queen Margherita di Savoia at the U.S. Embassy in Rome. *Analytica* 3 (2022): 406-429.
21. Chavazas M L, Berthonneau J, Payan C, et al. 3D damage imaging of Carrara marble sculptures by acoustic tomography coupled to photogrammetry. *Journal of Cultural Heritage* 73 (2025): 215-224.
22. Zheng L, Li K, Wang J, et al. Investigations on the surface deterioration process and mechanisms of white marble. *Construction and Building Materials* 472 (2025).
23. Sedek M S, Touahmia M, Albaqawy G A, et al. Four-Dimensional Digital Monitoring and Registering of Historical Architecture for the Preservation of Cultural Heritage. *Buildings* 14 (2024): 2101.
24. Fioretti G, Acquafredda P, Calò S, et al. Study and Conservation of the St. Nicola's Basilica Mosaics (Bari, Italy) by Photogrammetric Survey: Mapping of Polychrome Marbles, Decorative Patterns and Past Restorations. *Studies in Conservation* 65 (2020): 160-171.
25. Chanda P, Singh K, Aalam, U, et al. Comprehensive spectral and imaging studies of marble to assess the environmental damage using ULF Raman and THz absorption studies. *Optics for Arts, Architecture, and Archaeology IX* 12620 (2023).
26. Vagnon F, Comina C, Canepa M C, et al. Experiences and preliminary results of geophysical methods on historical statues. *Conf. Ser.: Earth Environ. Sci* 1124 (2023).
27. Anevlavi V, Prochaska W, Ruhland A S, et al. Tracing Material Origins: Provenance Studies of White Marble in Roman Temple E of Ancient Corinth Using Archaeometrical and Geoarchaeological Methods. *Minerals* 15 (2024).
28. F Matz. Antikensammlugen in England. *Archäologische Zeitung* 31 (1874): 21-36.
29. P S Parreira, F L Melquiades, F Lopes, et al. Sistema portátil de fluorescência de raios X (Patent: PI 0801331-4 B1).
30. IAEA. Quantitative X-ray Analysis System (QXAS) User Manual (1996).
31. Wold S, Esbensen K, Geladi P. Principal Component Analysis. *Chemometrics and Intelligent Laboratory Systems* 2 (1987): 0169-7439.
32. Härdle W K, Simar L. Cluster Analysis. In: *Applied Multivariate Statistical Analysis*. Springer, Berlin, Heidelberg (2015).



This article is an open access article distributed under the terms and conditions of the [Creative Commons Attribution \(CC-BY\) license 4.0](https://creativecommons.org/licenses/by/4.0/)